

## 2. ACCELERATOR AUGMENTATION PROGRAMME

### 2.1 LINAC

S. Ghosh, R. Mehta, G.K. Chowdhury, A. Rai, P.N. Patra, D.S. Mathuria, S.S.K. Sonti, J. Zacharias, B.K. Sahu, A. Pandey, P.N. Prakash, D. Kanjilal and A. Roy

#### 2.1.1 Development of New Drive Coupler

To change the coupling strength and couple the RF power into cavities we had a drive coupler based on rack and pinion design to facilitate linear motion of the loop. The Quarter Wave Resonators (QWR's) require nearly 300 Watts of RF power to generate field of ~4 MV/m in over coupled mode. Due to this high power requirement, in our first few tests, we found that the insulator of rf power cables were melting and a thin layer of material was deposited on to the cold surface of cavities. A detailed analysis of this thin film was done using Energy Dispersive X-Ray Analysis (EDX) at Solid State Physics Laboratory. This showed Zn (96.5%)/Cu (2.49%) in atomic % as main peaks. The rack and pinion were made of brass and the excessive heating during powering of the cavities might have caused the coating. A new drive coupler was designed to replace the rack and pinion and to also incorporate LN<sub>2</sub> cooling. Salient features of the new drive probe are:

- 1) The movement of drive probe is done using worm and worm wheel.
- 2) Liquid nitrogen cooled central conductor and outer conductor.

A cold test was undertaken to check the performance of the new drive coupler. High power pulse conditioning was done for long duration (4-5 hrs). Cavity was then locked at 2.2 MV/m @ 150-170 watts of input power for nearly 18 hrs. With successful completion of the test it was decided to replace all old drives with the new design. Process of fabrication and installation of new drive probes is over. To increase the coupling range a rotational motion was incorporated along with linear motion through a spiral groove. This enables the loop to have a linear travel of ~70 mm and 70° rotation. Figures 1 & 2 show the old and new drive couplers.



**Fig. 1. Old Drive Coupler**

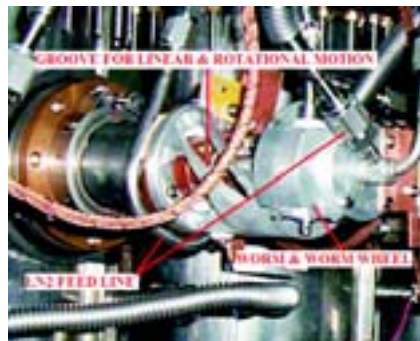


**Fig. 2. New Drive Coupler**

### 2.1.2 A Novel Technique of Reduction of Microphonics in Superconducting Resonators

During on-line beam tests of niobium superconducting quarter wave resonators (QWR), it has been observed that due to presence of microphonics in the ambience of linac, rf power of about 300 watts is required to lock the resonators in over-coupled mode. The high rf power causes several operational problems like melting of insulation of RF power cable; excessive heating of drive coupler leading to other associated problems and increased cryogenic losses. To reduce the requirement of RF power, a novel technique of damping the mechanical mode of the resonator by inserting stainless steel balls of suitable diameter inside the central conductor (figure 3) of the QWR has been adopted [1]. Due to dynamic friction between the balls and the niobium surface, the amplitude of the vibration of the central conductor excited by the mechanical mode has been reduced drastically. Microphonics measurement on QWR at superconducting temperature has been performed without/with SS balls with the help of cavity resonance monitor in phase lock loop and a reduction of microphonics by a factor of 3 has been recorded with balls as damper. During phase and amplitude locking, a remarkable reduction of input rf power of about 50% (figure 4) has been achieved to lock the resonator. This remarkable reduction of microphonics and input rf power has been repeatedly achieved during different cold tests of several resonators.

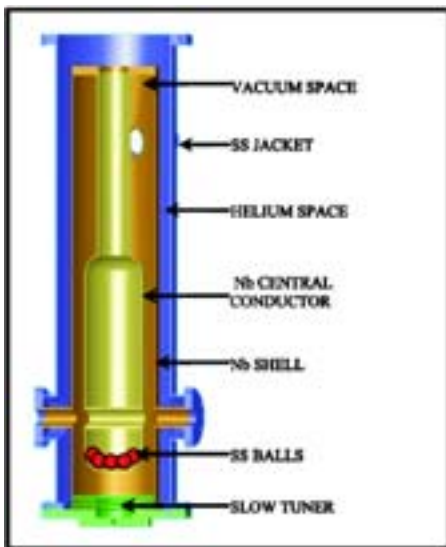


Fig. 3. Cross sectional view of resonators with a few SS balls

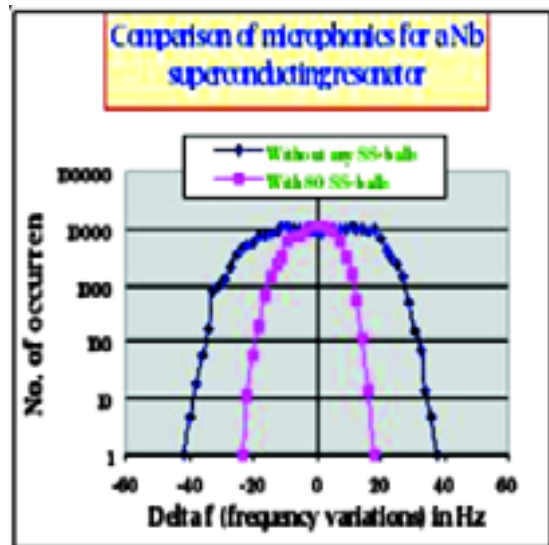
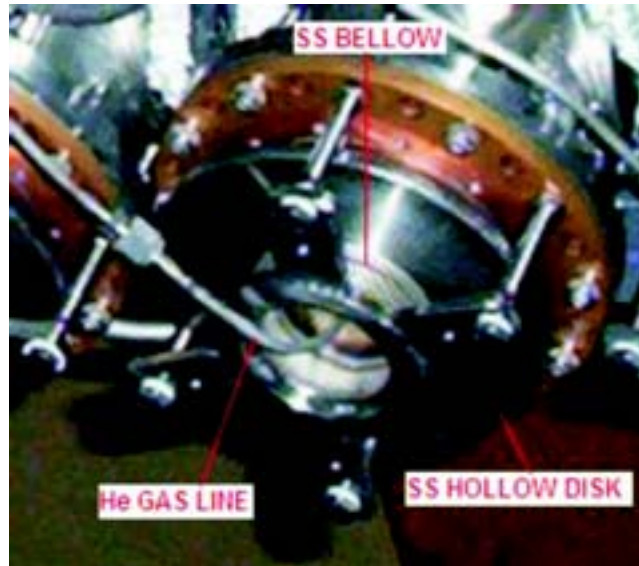


Fig. 4. Frequency excursion of a superconducting resonator with and without SS balls

### 2.1.3 Slow Tuner Development

During last few cold tests the original slow tuner bellows were observed to start leaking from welding joints. Though we were successful in our earlier efforts to modify

the slow tuner cover flange assembly to ensure leak tight indium joint, but due to welding cracks in niobium bellow we decided to re-design the whole system of slow tuner. Due to constraints from cryostat side and time schedule it was decided to use same niobium bellow and flexing technique but without introducing the He gas inside the niobium bellow. This design is now incorporated in first linac module. In new design He gas is introduced in SS bellow and through a mechanical attachment, linear motion is transferred to niobium bellow. The new design was successfully tested in STC for frequency range and response measurements. Figure 5 shows new slow tuner assembly.



**Fig. 5. New Slow Tuner Assembly**

#### **2.1.4 Improvement in LHe Cooling in Linac Cryostat and Off Line Tests**

For the linac module we require eight resonators. The coating of thin film on resonators surface were removed by light electropolishing of the resonators. It was observed in the past that performance of the resonators had deteriorated in linac cryostat in comparison to its performance in STC. To confirm these two resonators were tested in STC and linac respectively. Later, after the test, they were swapped with each other and tested again. This confirmed the degradation in the performance of resonator in linac cryostat as compared to its performance in STC. The cause of this deterioration seems to be due to the different ways of cooling the resonators. The SS top flange of the resonator is flat and clearance between this flange and top niobium surface is about 1/2 inch. During boiling of liquid helium bubble may get trapped in this region. In linac cryostat the SS top flange of the resonator is connected to liquid helium dewar through an SS bellow of internal diameter of ~ 1.5 inch whereas in STC this joint is made through an adapter flange of inter diameter of ~4 inch. To overcome this, a HAT like structure having slope for movement of bubbles and as well as a buffer volume is developed. Figure 6 & 7 shows the linac cryostat without and with HAT. This HAT structure gives two fold advantage,

one it provides a buffer volume for LHe, secondly it does not allow bubble to be trapped, thus localized heating / insufficient cooling problem is removed. Results of performance tests with HAT type structure showed marked improvement. At present all eight resonators in linac cryostat are connected to liquid helium dewar using this HAT structure.

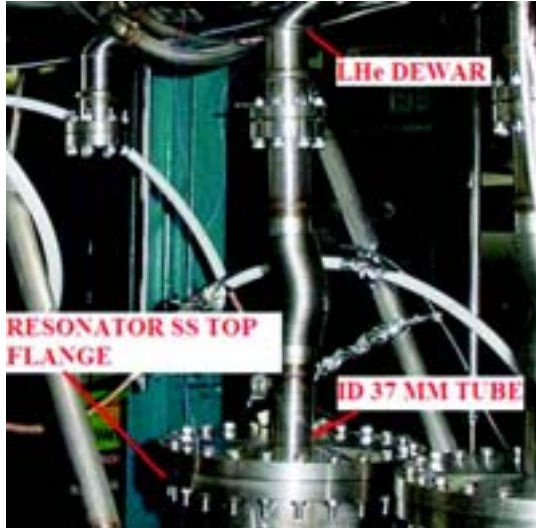


**Fig. 6. Without HAT Structure**

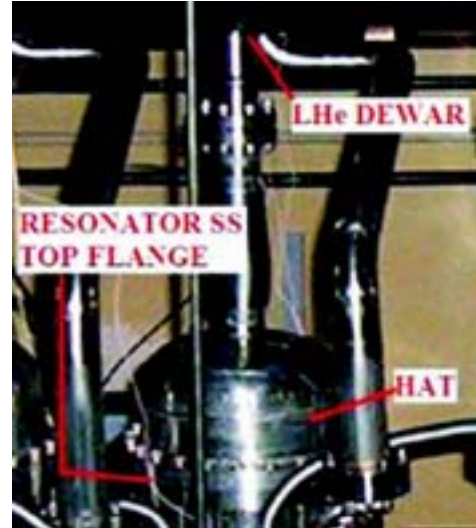


**Fig. 7. With HAT Structure**

With the following improvements incorporated in linac cryostat (see figure 9),

- 1) New design of drive coupler
  - 2) Modified slow tuner assembly
  - 3) HAT structure to create LHe buffer volume for better cooling rate
  - 4) SS balls were inserted in central conductor (drift tube) for damping,
- we are now ready for off line test followed by beam test with all the eight resonators.

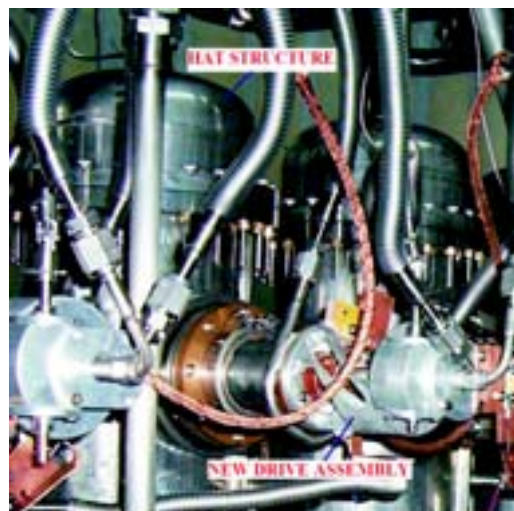


**Fig. 8. View of HAT and New Drive Coupler Assembly**



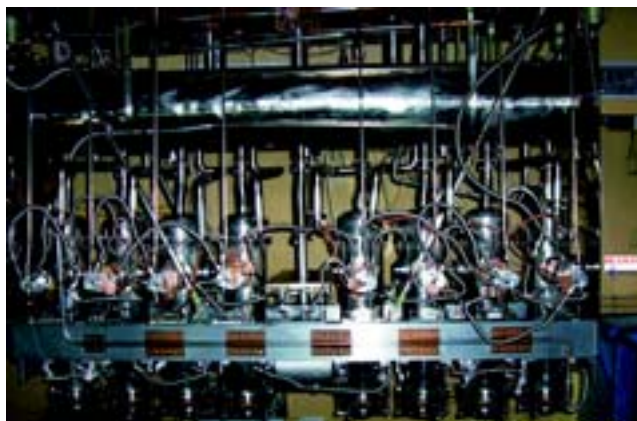


**Fig. 9. Full View of Linac Cryostat**

### 2.1.5 High Pressure Rinsing Facility

A high pressure rinsing (HPR) system has been designed, fabricated and commissioned at NSC. The rinsing system has been installed in a class 100 clean room with a SS304 tank for waste water disposal. Figure 10 shows main components of the high pressure rinsing system. The details of the nozzle design are given in Figure 11. Figure.12 shows the photograph of the high pressure rinsing system. After commissioning of high pressure rinsing system, several trial runs were performed. During the test runs it was observed that small particulates of carbon were deposited on the micron filter membrane. It was also noted that the SS DI water tank and SS pipes were also rusted from inside. With nozzle assembly being fixed it becomes difficult for cleaning of nozzle holes whenever they are clogged due to the scaling.

It was decided to modify the assembly to make the system ultra clean for rinsing the niobium QWR's [2]. For efficient cleaning and easy replacement of the nozzle assembly, the nozzle head was made de-mountable. Following three major modifications were undertaken

- (1) Nozzle Assembly made de-mountable.
- (2) Entire SS pipe line chemically treated to remove rust and scaling.
- (3) SS over head tank for DI water storage was replaced by a HDPE water tank.

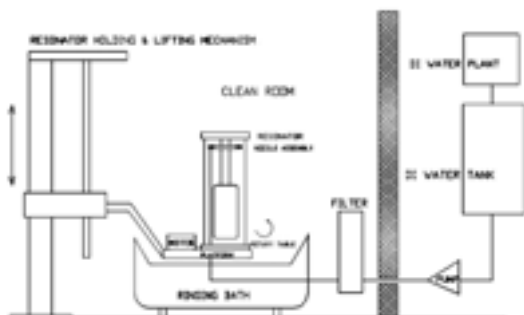


**Fig. 10. Detailed Drawing of HPR System**

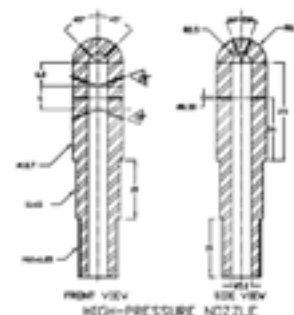


**Fig. 11. Nozzle Assembly**



**Fig. 12. HPR System**

## REFERENCES

- [1] "A Novel Technique of Reduction of Microphonics in Superconducting Resonators", S. Ghosh, R. Mehta et al, 10<sup>th</sup> International Conference on Heavy Ion Accelerator Technology, Port Jefferson, NY.
- [2] "Modifications of High Pressure Rinsing System", S.S.K.Sonti et al, Technical Report IUAC/TR/SSKS/2005-2006/19

### 2.1.6 Fabrication of Superconducting Niobium Resonators

P.N. Prakash, S.S.K. Sonti, K.K. Mistri, J. Zacharias, D. Kanjilal & A. Roy

The first completely indigenously built quarter wave resonator has been tested successfully. Production of fifteen more resonators for the second and third linac modules has progressed well. In addition, several resonators with leaking coupling port bellows have been repaired.

#### 2.1.6.1 Successful Testing of Completely Indigenously Fabricated QWR

The first completely indigenously fabricated quarter wave resonator (QWR) [1] was tested along with its slow tuner bellows. In cold tests the low field weakly coupled decay time was measured to be better than 5 seconds corresponding to a  $Q_0$  of  $1.5 \times 10^9$ . Due to shortage of liquid helium during the test the resonator could not be fully conditioned with the high power RF amplifier. However, with very little conditioning the resonator

could easily operate at 3.5 MV/m with 3.5 W RF power. The slow tuner range was measured to be 70 kHz for a pressure change of 20 psi. The successful testing of the first indigenously built QWR provided the confidence to undertake production of resonators for the 2<sup>nd</sup> and 3<sup>rd</sup> linac modules.

#### **2.1.6.2 Resonator Production for the 2<sup>nd</sup> & 3<sup>rd</sup> Linac Modules**

Production of fifteen QWRs for the 2<sup>nd</sup> and 3<sup>rd</sup> linac modules began in mid 2005 and we plan to complete the construction in two years time. So far about 20% of the work has been completed. Fabrication of the niobium outer housing assemblies of all the resonators is nearing completion. In addition, machining of the niobium-stainless steel composite flanges and fabrication of the loading arms (inductive part of the quarter wave central conductor) has been completed. Machining of several other parts such as the drift tube beam ports is being done. The electron beam welding is being performed in batches to enable several welds to be done in a single pump down.

#### **2.1.6.3 Repairing of Coupling Port Bellows**

On several resonators the leaking long coupling port bellows assemblies were repaired by machining them out and replacing with a new assembly. Some resonators had leaky bellows in the short coupling port. They were machined out and the ports were blanked off. In all five ports on five different resonators were successfully repaired.

#### **2.1.6.4 Modification of a QWR to Study Multipactoring**

The existing QWR suffers from severe two point multipactoring and the resonator takes between sixteen to twenty hours to condition through the low level barrier. This is due to the drift tube-outer housing gap (3.35 cm) and the RF frequency (97 MHz), the combination of which results in the electron energy (proportional to the square of both the gap and the frequency) very near the maximum secondary electron emission coefficient of niobium. The large surface area of the drift tube cylinder (twelve inches long), which is concentric with the outer housing, makes it worse. By reducing the drift tube diameter, thus increasing both the drift tube-outer housing gap (to 4.13 cm) and the resonance frequency (to 109 MHz), the electron energy would go closer to the upper crossover limit on the secondary electron emission curve. It is therefore logical to expect that such a geometry would condition through the low level multipactoring barrier quickly. The length of the drift tube remains unchanged in order to retain the same overall height of the resonator so that the same housing can be used for modifying the geometry. Numerical simulation was done using SUPERFISH to check the RF frequency and the peak surface fields. Although we do not foresee using this structure in our linac we have chosen the RF frequency to be a multiple of the pre-tandem buncher frequency.

In terms of hardware three new die/punch sets and couple of machining and welding fixtures are required. The effort and cost of this is nominal. We have already made some trial dies and at the time of fabricating the drift tubes for the production resonators we will fabricate the parts for the 109 MHz structure also.

## REFERENCES

- [1] Nuclear Science Centre Annual Report 2004-05, p17

## 2.2 CRYOGENICS

T.S. Datta, J. Chacko, A. Choudhury, J. Antony, M. Kumar, S. Babu, S.A. Krishnan, S. Kar, R.S. Meena, R.G. Sharma and A. Roy

In this academic year, seventeen cold tests have been performed for resonators in off-line and beam line cryostats. The rebuncher cryostat with cavity has been successfully integrated with the helium distribution network and performance was found to be satisfactory. Indigenously developed speed -controller for the cold expansion engine has been incorporated with the cold box. A series of experiments have been carried out in MLI test set up. Many new activities like development of superconducting solenoid magnet, S.C. quadrupole magnet and performance studies of gravity cooling have been initiated in this period. Many electronics devices like temperature monitor for the DT-470 Si- diode, Pt-100 and digital monitor for different gas flowmeter have been developed.

### 2.2.1 Cryogenic Facility

#### I. Liquid Helium Plant:

The helium plant was operated 17 times and out of which only five runs were in close loop mode for off-line testing of the resonators in Linac and rebuncher cryostat. Estimated total production of LHe was ~ 60000 L which is less in comparison to last year as majority of the runs were in open loop mode. Fincor controller, which controls the speed of the cold engine was having problem for last two years. A stop-gap arrangement was made by dissipating the power generated by engine in a series of room heater. A permanent control box with many additional features has been developed and integrated with helium refrigerators. Performance is satisfactory and a similar one is being planned for the warm engine.

The oil- free Haug compressor is being operated regularly during off-line testing of cavity in STC resulting in power saving (to the tune of 75KW X 200hrs) last year.



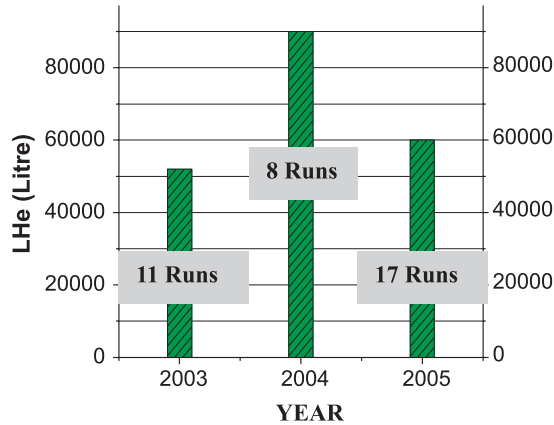


**Fig. 1. Bar Chart of LHe Production**

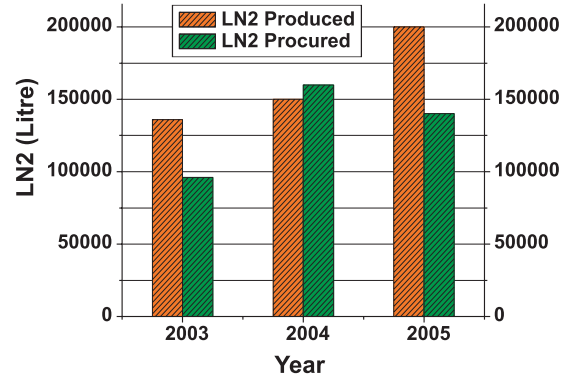


**Fig. 2. Bar Chart of LN2 Production**

## II. Liquid Nitrogen Plant:

The plant was operated for 4000Hrs and estimated liquid nitrogen production was 2,00,000 L which is significantly higher than last two year which is shown in the fig.[2]. LN2 procured from outside vendor was ~1,40,000 L. To increase the in house production rate from 50L/Hr to 150L/Hr, different options of flow scheme with different configuration have been analyzed. Finally it has been decided to run the plant in semi-closed loop with both cryogenerators. PSA capacity will be augmented to meet the demand of extra gas. Order has been placed for the same and expected to be installed by middle of this year.

## III. Helium Gas Purifier and Recovery System:

The indigenously developed helium gas purifier has been operated successfully for ~50 Cycles and approximately 5000M<sup>3</sup> of helium gas has been purified. The new high pressure impure helium gas tank (2500L water volume and working pressure ~120bar) has been commissioned and integrated with the recovery network.

### 2.2.2 Performance Report of Cryostats

In the Linac cryostat, three off line tests with 3-4 QWRs have been performed in this academic year. One nude-ion gauge has been installed parallel to the cold cathode gauge in the cryostat to monitor the vacuum profile during LHe cooling. Figure [3] shows the clear indication of vacuum improvement upto 5E-9mbar at 4.2K which was earlier not shown by the cold cathode gauge. Close loop cooling of Linac cryostat is achieved with minimum human interference by reducing JT pressure.

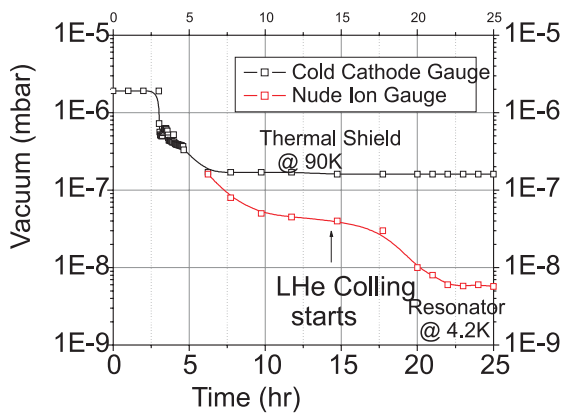


**Fig. 3. Vacuum profile during LHe Cooling**

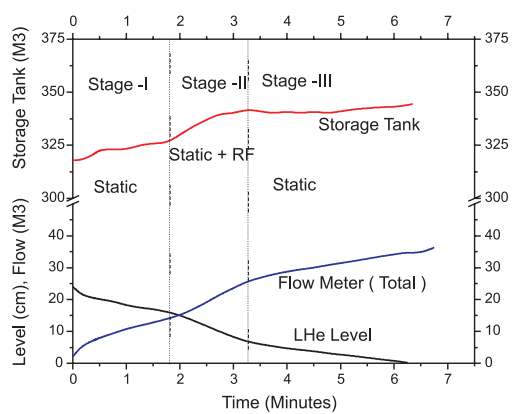


**Fig. 4. Dynamic Load Verification test**

Eight cold tests have been performed in Simple test cryostat (STC). Among them one test was dedicated to verify the real dynamic RF power which goes to the liquid helium during the RF performance test of the resonator in this cryostat. The RF power ( $\sim 6W$ ) given by the amplifier to the resonator has perfectly matched with the evaporated helium gas which is shown in fig.4. It is also observed that multipactoring does not reappear once the resonator is forcefully warmed up to 100K and then cooled down to 4.2K.

Cold tests in the rebuncher cryostat were performed first time this year using LHe cryonetwork. To have faster cool down rate, the evaporated helium gas was forced to circulate through the precooling channel of the resonator. Once the temperature of the resonator reaches 20K, the flow is diverted. The same methodology of precooling might be followed in the 2<sup>nd</sup> Linac module. The static heat load of the cryostat is measured to be  $\sim 13W$  at 4.2K. Figures 5 and 6 show the cooling profile and the static load measurement respectively.

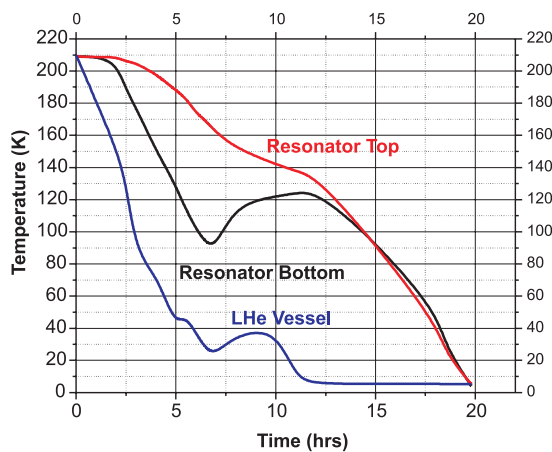


**Fig. 5. LHe cooling of Resonator in RBC**

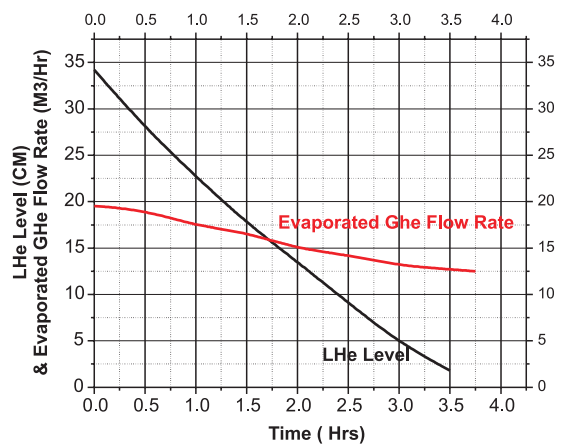


**Fig. 6. Static heat Load Measurement of RBC**

## 2.2.3 Other Experimental Studies

### I. MLI Set Up

Based on our earlier observation of funneling of angular radiation from the top plate, the existing calorimeter has been modified by incorporating additional liquid nitrogen vessel on top of upper guard vessel. With this modified version the residual load (80K – 80K) is reduced from 360mW to 40mW.

A series of experiments have been performed to measure heat load between 80K and 4.2K with various layers of MLI, Al tape and with bare metal surface. A datasheet with the temperatures recorded is shown in fig [7]. A joint collaboration project between IUAC and Wroclaw University of Technology, Poland has been initiated to study the detailed performance of aluminium tape as an alternative cryogenic insulation. This project is jointly funded by DST and Poland Academy of Science. A mathematical model on heat transfer is proposed to validate the experimental data.

### II. Gravity Cooling (Thermosyphon Cooling) Set Up

The thermal shield of the buncher cryostat is being cooled by using thermosyphonic effect. It has been observed that the shield temperature increases with downfall of liquid level in the dewar. An experimental set-up has been developed to understand this phenomenon so that a more efficient mechanism for cooling the shield is present. Number of measurements has been carried out with different load and for two different configurations. More data are being collected.

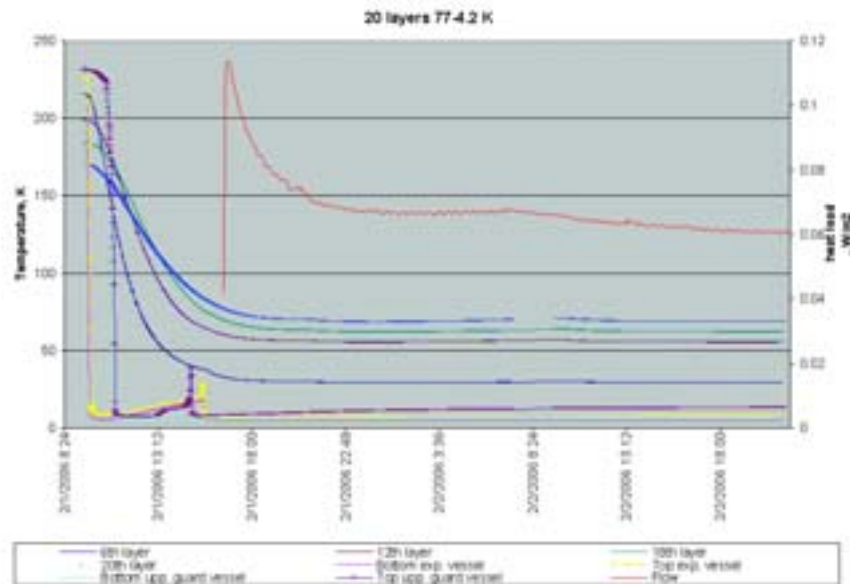


Fig. 7 Test Results of MLI experiments

## **2.2.4 Other Developments**

### **I. Arc Cell Nitrogen Detector**

An arc cell has been developed which detects the presence of trace amounts of nitrogen gas impurity in helium stream in the 0-80 PPM range. This module replaces the existing module where a monochromator is being used to detect the light output.

The gas stream for which impurity has to be tested is injected as to a SS cube through a regulator which controls the flow rate and pressure. A flow meter (on the inlet side) is used to measure the rate and a 1 PSI relief valve of appropriate Cv is used at the outlet side. The actual flow is ~0.4 SCFH and the regulated pressure is ~1PSI in the cell. This cell is connected to a high voltage DC power supply (2KV, 15mA ) to generate the arc and the arc current is controlled with the help of some aluminium-clad resistors (120Kohm, 150 watt) which are cooled with a fan and put in series to the supply. Once the arc is produced, corresponding light is selected through an optical filter (356nm) and the UV enhanced photodiode detects the light. One signal at 355 nm corresponds to nitrogen excitation line (which has a combination of both neutral and singly ionized nitrogen states) in helium gas. This light signal is then amplified with an amplifier (gain  $10^9$ ) and fed to a linearized display which shows the concentration of nitrogen in PPM. This unit has been in operation for the last couple of months and is actively controlling the helium gas purifier output set level at 100 ppm.

### **II. Superconducting Solenoid Magnet**

A 7 Tesla insert type superconducting solenoid magnet has been designed and developed to have hands-on experience of superconducting magnet technology. It has three major components (1) Solenoid magnet (2) Vapor cooled current leads (3) Support Structure. Two vapor cooled leads have been developed to carry ~250A of DC current. This magnet is used as an insert in a LHe container of 100mm neck diameter. After training, the magnet achieved the field ~ 7.1Tesla at 215 A. The magnet was charged using three indigenously developed power supplies (SMPS of 100A @10V) in parallel. The quench protection system performed well during the quench at 6.2Tesla. Field value with respect to current is shown in fig. [8] and fig. [9] show the axial field profile.



Parameters of S.C. Solenoid Magnet		
1	Working Bore	46mm
2	Outer Winding Diameter	83mm
3	Winding Length	150mm
4	Conductor Used	0.75 mm Cu/ Nb-Ti
5	Copper : SC Ratio	1.8:1
6	No. of Filaments	45
7	Filament Diameter	38 Micron
8	No. of Turns per Layer	200
9	No. Of Layers	22
10	Total Conductor Length	0.9 Km
11	Interlayer material	Fiber Glass
12	Impregnation Material	Bees Wax
13	Inductance Of the Magnet	0.4Henry
14	Field At 210 Amp	7.1 Tesla
15	Stored Energy at 210 A.	8.8KJ

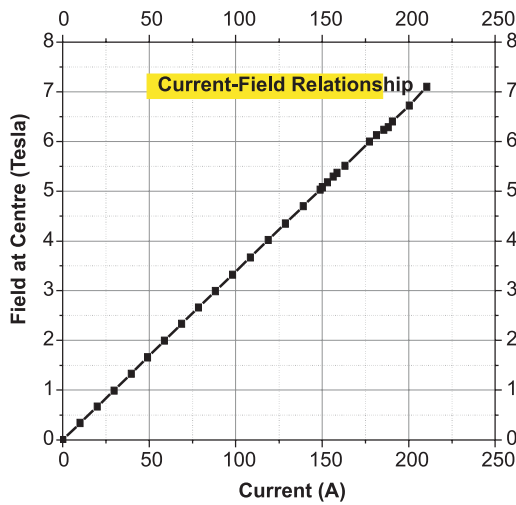


**Fig. 8. Current – Field Relationship of 7 Tesla S.C Solenoid Magnet**

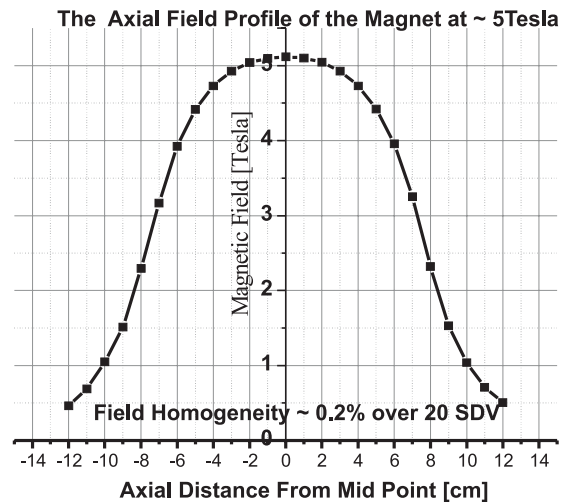
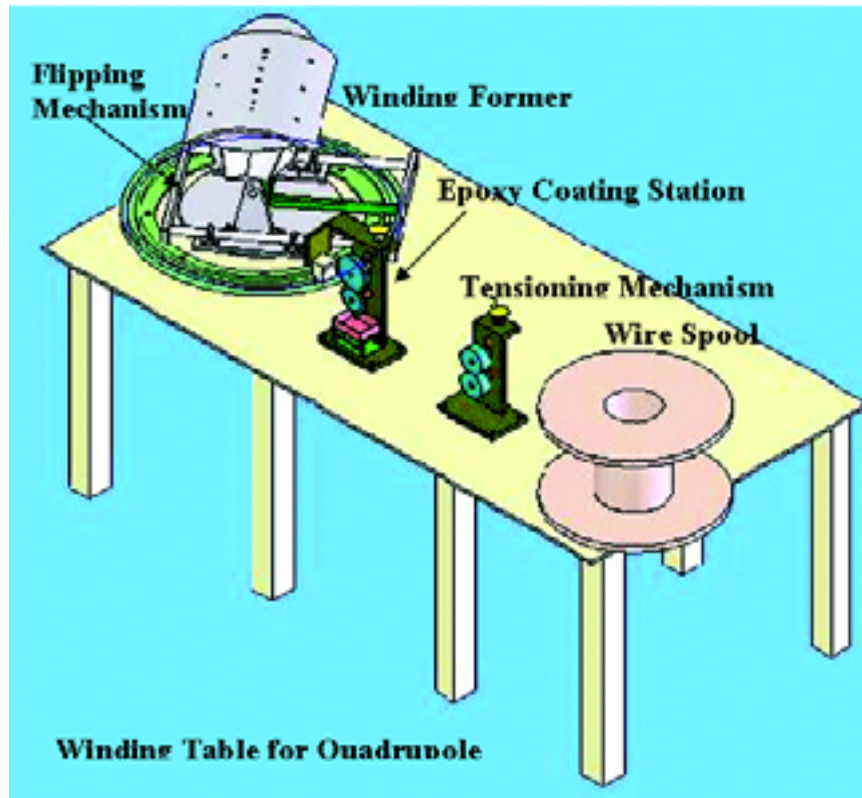


**Fig. 9. The axial field profile of S.C. Solenoid Magnet at 5 Tesla**

### III. Superconducting Quadrupole Magnet

A superconducting quadrupole magnet is being designed and developed for the HYRA project. Two quadrupole magnets of same warm bore and different length will be assembled in a single cryostat. Pole length of first magnet (Q1) is 300mm and second magnet (Q2) is 250mm. The magnets will be placed 200mm apart. Yoke dimensions of

Q1 are OD780, ID 490 and thickness 300. Yoke dimension of Q2 is OD 780, ID 490 and thickness 250. Q1 will have maximum field of 2.2T at the pole tip and Q2 will have 1.75T at pole tip. To get the desired cross sectional shape of the coil, a winding former is designed and it is under fabrication. A winding table with a flipping mechanism is required to achieve the specific shape of the coil and it is under design. Yoke and pole tips fabrication is under progress.



To have higher storage capacity for liquid helium and to have flexibility on opening the magnet, rectangular shape vacuum jacket is preferred over cylindrical shape. Conceptual design of cryostat has been made and the sketch is shown in fig. [10].



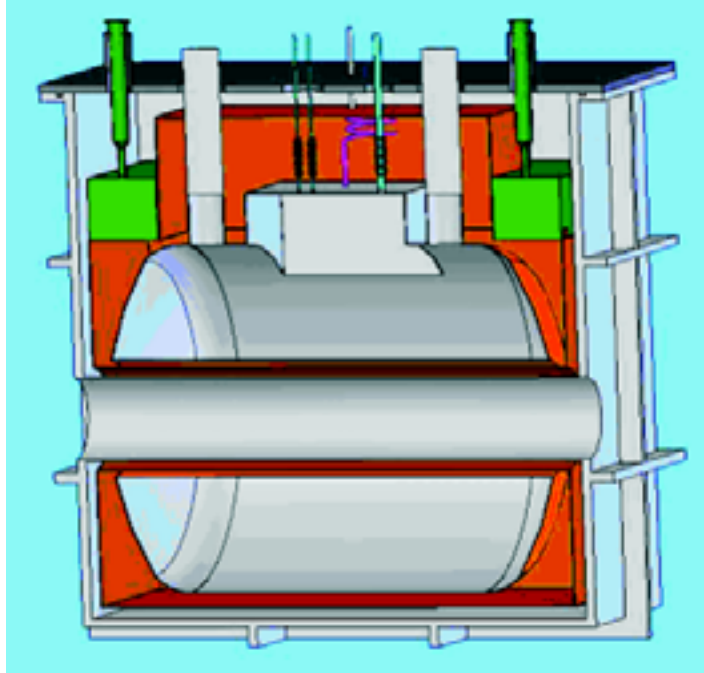


**Fig. 10. Conceptual design of S.C. Quadrupole cryostat**

## **2.2.5 Cryogenic Instrumentation other Electronics Development**

Joby Antony and D.S. Mathuria

### **I. Minimizing the errors due to RF pickup of LINAC Thermometry**

After many experiments to minimize the RF fluctuations in LINAC thermometry, the problem has been reduced successfully to its minimum by doing the following things in combination

1. The complete cabling inside three cryostats, viz., LC-I, RBC, STC were modified with tight twisted thin 12 Twists pair per inch SPHSCA wires for better rejection of common mode signals
2. RF bypass condensers were connected at every soldering points inside cryostats
3. Copper caps were put around diode sensors to reduce RF penetration
4. Additional Low pass filter circuit was used for signal conditioning.

### **II. Gas Flow counter with RS232 O/P**

An electronic unit has been designed and developed to readout the gas flow in  $\text{m}^3/\text{hr}$  to use with M/s Krom Schroder BK-G2.5 mechanical Diaphragm gas meters fitted with a Low-frequency pulser IN-Z31. The electronic unit can be used for experiments to

handle flow rates from 4 m<sup>3</sup>/hr down to 0.01 m<sup>3</sup>/hr along with total accumulated flow of maximum 40.95 m<sup>3</sup> since a previous reset. The display values are read into a PC using RS232 using a small logging program.

Some of the design parameters are :

- FPGA based design
- VHDL UART implemented in OPTO-isolated RS232 protocol
- 16\*1 HD44780 compatible display interface in VHDL



**Fig. 11. Pt -100 Temp. Monitor [73K-410K]**



**Fig. 12. Digital Gas Flow Meter**

### III. A 73-410K precise Cryogenic Temperature monitor for Pt-100 sensor

An instrument has been designed for temperature measurements in the range of 73 to 410 K. The instrument uses class-A type PT100 RTD as the temperature sensor which is excited by a current of 100  $\mu$ A (to reduce self heating) and displays T in Kelvin with accuracy better than +/-0.2K. The non-linear resistance-temperature variation of PT100, which a third order polynomial, is implemented digitally inside a Xilinx FPGA chip using interpolation to read T in Kelvin. The device reproduces a digitally linearized 4-20 mA current loop and 0-10 Volt DC output for data acquisition.



**Fig. 13. DT470 Si diode Temperature Monitor [ 3.2-410K]**



**Fig. 14. Temperature Monitor [0-100°C]**

Similarly a 0-100°C Temperature monitor with a 0-10V /4-20 mA O/P between 0 and 100°C is also developed for acid temperature measurements in surface preparation lab.

#### **IV. A precise 3.2K to 410K Cryogenic Temperature Monitor for Si-diodes**

A precise low Temperature monitor (3.2K-410K) for very low temperature measurements has been designed and developed. The instrument uses DT-470 silicon diodes ( manufactured by Lakeshore Cryotronics) as the temperature sensor and displays T on a character display to get a display -accuracy of T better than +/-0.01K below 10 K and +/- 0.1K above 10K. The non-linear voltage-temperature variation of DT-470 (Curve-10 standard curve) is implemented digitally inside a Xilinx FPGA chip using interpolation to read T in Kelvin. The device reproduces a digitally linearized 4-20 mA current loop and 0-10 Volt DC output for interfacing to the control systems. A VHDL UART is implemented to provide an optically isolated RS232 interface. The FPGA software is implemented as an FSM using VHDL inside a single chip. The device has been tested for its long term stability.

#### **V. Impurity Monitor display meter with 4-20mA for controls**

A 0-100 PPM meter is used to display impurities in helium. The sensor will give 0-100 mV non-linear input and output is linearized 4-20mA which is directly proportional to PPM.

#### **VI. Gamma Ray Display Monitor**

A 0-100  $\mu$ A linear input signal is conditioned to display 0-40mR of gamma radiation in logarithmic scale with 0.01mR display resolution and linearized outputs of 0-10V/4-20mA. (PC board assembled and tested by health physics personal, design &FPGA implementation by us)



**Fig. 15 Gas-impurity Monitor (PPM)**



**Fig. 16 Gamma-radiation Display**

## **VII. Other Accessories**

Thermal mounts, LN<sub>2</sub> sensor etc. New prototypes of Thermal mounts, LN<sub>2</sub> sensor are designed and tried out. Experiments are awaited.

## **VIII. EBW Control System**

This year there was a major breakdown of CNC system of EBW. After through troubleshooting it was found that the partition and parameters of CNC computer has been corrupted due to aging of the battery backing up a EEPROM. The problem was solved and made it ready for operation.

### **2.3 RF ELECTRONICS**

A. Sarkar, S. Venkataramanan, B.K. Sahu, K. Singh, A. Pandey, Y. Mathur and B.P. Ajith kumar,

#### **2.3.1 Status Report of the Multi-harmonic Buncher & the High Energy Sweeper and associated jobs**

The multi-harmonic buncher (MHB) was operated along with the high energy sweeper (HES) for the first time to provide 12 MHz pulsed beam to a Pelletron user (Hardev Singh of Punjab University). Earlier this system (MHB+HES) was used to provide beams only to the Linac. <sup>16</sup>O beam pulses with FWHM ~1ns was provided to the user. The sweeper slit was optimised and kept at 2mm. The sweeper phase had to be tuned occasionally to get the beam back. The entire system ran smoothly for several shifts.

The multi-harmonic buncher (MHB) was also operated along with the low energy chopper (LEC) to provide 4 MHz pulsed beams to HIRA beamline ( User: S.Pravin of Bangalore University) and GDA beamline ( User: Vivek Kumar of Punjab University). In both these runs <sup>16</sup>O beam pulses with FWHM ~ 1ns was given. Travelling Wave Deflector (TWD) was also used in the HIRA run to provide pulsed beam at lower repetition rate. This system (MHB + LEC) was also used to provide the first beam to beam hall II (GPSC II) for the facility tests of Neutron Detector Array. Using this system <sup>19</sup>F pulsed beam was provided to the Punjab University group for a very long run of 15 shifts. During this run the chopper phase had to be adjusted occasionally (after power cuts and glitches) to bring the beam back on target.

All the above mentioned pulsed beam runs were given with the phase detector cavity in the new position i.e. before the faraday cup (FC-04) and sweeper slits in the vault area. Earlier the phase detector was after the sweeper slits. The advantage of the new phase

detector position is two-fold. Firstly, loss of beam from target due to sweeper phase change or improper sweeper slit window did not have any effect on the beam phase lock. Moreover the beam phase lock remained intact even with beam stopped in FC-04. This helped a lot during pulsed beam tuning. However, since the level of beam currents and beam trajectories were different in the current position of the phase detector compared to that in the previous position, the gains of the controller and delays to the master clock driving the buncher had to be adjusted to get back the proper phase lock.

During the last pulsed beam run, it was observed that the flow of the de-ionised water in the closed loop cooling system for MHB was reduced considerably. The tank circuit lid for the MHB was opened and the coils were cleaned thoroughly using compressed air. Two major leaks were identified in the water tubes running between the coils. These tubes were replaced with fresh ones. Other joints were also tightened. Fresh de-ionised water was filled in the system. The coils were tuned and checked with high power.

During the high energy sweeper operation it was found that to tune the tank circuit, the capacitors had to be operated almost in the extreme out position. This was not a very favourable condition for long term operation of the sweeper. The tank circuit coil was stretched slightly to decrease the inductance of the coil. This helped to tune the tank circuit in the required frequency (6.0625 MHz) with the capacitors at the mid positions. One of the two pumps running the de-ionised water to the sweeper tank circuit coil was not working. This pump was removed, repaired and restored back into the system.

### **2.3.2 Status of Resonator control Scheme**

The Resonator Control modules are being used extensively for the testing of Linac resonators in Simple test cryostat and Linac cryostat. The next set of Linac resonator control modules for second Linac cryostat is being made this year and tested. The delta F circuit is being modified for automation of resonator locking. It has been tested first in the new set of resonator control module and then being changed in the old ones. This delta F control is tested and found to be working satisfactorily. The production of CAMAC modules for resonator control modules are over.

The slow-tuner mechanical assembly with new rated proportional valve is being tested extensively with different cavities and found to be working properly. The production of more numbers of slow-tuner mechanical assemblies using the same valve is going on. The earlier developed pot assemblies are working satisfactorily. Two more slow-tuner electronics modules consisting of eight channels are being fabricated and tested.

### **2.3.3 RF Power Amplifier for LINAC**

In house production of 10 units of VHF Power amplifier (97MHz, 400 Watts) for Linac having all necessary control and status read back circuits was initiated and completed

successfully. The amplifiers were burn-in tested for a week time continuously and characterised. We have also initiated in house production of 20 such amplifiers.

## 2.4 BEAM TRANSPORT SYSTEM

A. Mandal, Rajesh Kumar and S.K. Suman

Beam Transport System takes care of regular maintenance, design and development of beam Transport System of the Accelerators in the centre. This year we have developed a large area magnetic scanner and its power supply in the laboratory. Besides we have developed some special high voltage power supplies for solid state detectors. All the magnets installed in BH-II have been properly wired for energising power and tested offline locally as well as remotely from control room. The various beam diagnostic components have been wired for local as well as remote control. The performance of the whole beam transport system has been tested online with beam from Pelletron and was found to be satisfactory. Beam from pelletron was delivered for the first time to two beamlines (GPSC and MAT. SC.) for performing experiments. The details of the individual developments are described in this section.

### 2.4.1 Design of a large area Magnetic Scanner

A magnetic scanner has been designed for homogeneous irradiation of large area targets for material science beam line in BH-II. The scanner has a capability of scanning beam over an area of  $25 \times 25 \text{ mm}^2$  for beam of 400 a.m.u MeV at a distance of three metres at a frequency of 50 Hz. The scanner consists of two H-shaped dipole magnets; one for vertical and the other for horizontal scanning. They are placed one after other so that magnetic fields are perpendicular to each other. The yoke and poles are made of laminated silicon cores to minimise hysteresis loss. It has two halves and has been designed in such a way that one half can be taken apart to mount it on the beamline. The coils are made of solid rectangular copper conductor and designed for normal radiation cooling. The specifications of the magnets are as follows:

Shape	=	H
Pole gap	=	53 mm
Maximum field	=	1200 Gauss
Number of turns per coil	=	48
Inductance for two coils	=	~ 4mH
Conductor size	=	$8.12 \times 3.55 \text{ mm}^2$
DC resistance of each coil	=	
Current	=	50A
Output voltage at 50 Hz	=	60 V



The magnets have been fabricated by a local vendor under our supervision. The magnet is now ready for test.

#### **2.4.2 Design of an Air cooled Quadrupole Magnet**

Beam Optics calculation reported last year shows that the introduction of a short magnetic quadrupole doublet between ECR and Analysing magnet helps to improve the acceptance of the Analysing magnet. Accordingly a small air cooled magnetic quadrupole doublet lens has been designed. The magnet has been designed to take minimum space and minimum weight. Specifications are as follows:

Max. field gradient, g	=	2.6 T/m
Aperture radius	=	39 mm
Pole tip field	=	0.1T
Effective length	=	156 mm
Power for single Quad	=	100 W
Power supply	=	5V,20A

The hardware design of the magnet is going on.

#### **2.4.3 High Current High Stability Power Supply (300A/100V, 10 ppm)**

Rajesh Kumar, Raj Kumar, Bishamber K., S.K. Suman and A. Mandal

A 300A/100V, 10ppm linear current regulated power supply was under development since last year. This year final product has been assembled and handed over to HYRA group. This power supply has been designed for HYRA dipole magnets. The power supply has the following specifications and performance.

Specifications:

Stability	:	10ppm/ 8hrs.
Power range	:	30kW
Current range	:	300A
Voltage range	:	100V

Performance:

All drift and regulation data are given for maximum current output.

Drift (long term 8 hrs)	:	10ppm
Line regulation (10% change in line)	:	1ppm
Output ripple	:	20mVpp
Output polarity	:	Unipolar
Current setting	:	16 bit (4.5mA)



**Fig. 1. High Current High Stability Power Supply**

#### **2.4.4 High Current Scanner Magnet Power Supply**

S.K. Suman, Rajesh Kumar and A. Mandal

Beam scanning magnets are used to scan ion beams on targets over large area. The power supplies for these are AC amplifier which can provide current regulated triangular wave. The power supply has been developed with following specifications and features.

Triangular wave current output : 50A  
Output voltage range : 50V  
Scanning frequency range : 0 to 100Hz (4mH inductive load)  
Bandwidth (resistive load) : 10 kHz.  
Triangular wave current regulated output without cross over distortion  
Programmable foldback limits for over voltage and over current  
Remote control through CAMAC



**Fig. 2. High Current Scanner Magnet Power Supply**

The prototype power supply was developed last year to check the feasibility. After successful testing, an actual power supply has been developed this year with safety interlock, local and remote control operation.

#### 2.4.5 Programmable 5kV/100uA Ge detector bias Power Supply (NIM based)

Rajesh Kumar, S.K. Suman and A. Mandal

A programmable NIM based 5kV bias supply has been developed for germanium and silicon detectors. It can be used with any detector that can draw less than 100uA and whose gain is insensitive to the applied voltage. The regulation is done by SMPS technique and high voltage is generated by Cockroft-Walton multiplier.

Specifications:

Output Voltage range	: 0 – 5kV
Rated output current	: 0 – 100uA
Output stability	: < 0.1%
Noise and ripple	: < 10mVpp.

Features:

- Irrespective of setting output always ramp from zero.
- Needs a reset to put ON even if the power switch is ON.
- Output ramp up and Down facility.
- Output can be paused while ramping
- Over current protection.
- Ready signal after set output achieved.
- Polarity reversal by changing daughter board position.

This year a modified, finished and final product has been developed. Thirty five such power supplies will be fabricated for INGA project.



**Fig. 3. NIM based 5kV Ge Detector Bias Power Supply**

#### 2.4.6 400Vpp High Voltage Amplifier

S.K. Suman, Rajesh Kumar and A. Mandal

A high voltage amplifier has been developed using discrete components (low voltage op-amp and high voltage transistors) to drive the piezo crystals in STM. It replaces

the commercially available high voltage op-amp which is costly. The amplifier amplifies both DC and AC signals with the programmable gain.

Specifications:

Output Voltage : 400Vpp  
Rated Output Current : <5mA  
Frequency Bandwidth : 5kHz  
Gain : 20



**Fig. 4. 400Vpp High Voltage Amplifier**

#### **2.4.7 Local control panel for indigenously developed magnet power supply**

S.K. Suman, Rajesh Kumar and A. Mandal

Control panel electronics has been developed for operating indigenously developed power supply. It is a local user interface module for the power supply. The main functions of the module are for output current setting, power supply status/interlock display, output on/off control, Remote/locale control mode selection and a LCD panel meter for monitoring output voltage, load current and collector emitter voltage.

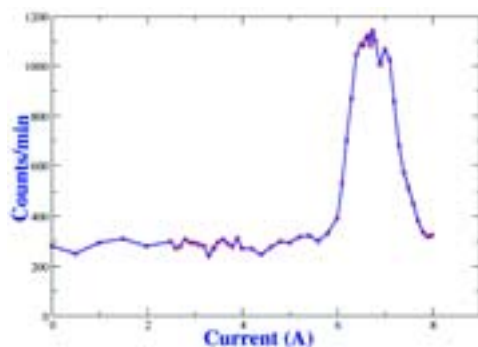


**Fig. 5. Local Control Panel for Magnet Power Supply**

## 2.4.8 Design of a Beta – Spectrometer

A. Mandal, S.K. Saini, Rajesh Kumar, S.K. Suman and S.K. Datta

A beta spectrometer has been developed for PG teaching lab. This consists of a solenoid magnet which selects beta rays of particular energy from a source and focuses on to a detector. The source and detector are housed in a SS chamber of 1.1 m long. The system operates in vacuum of  $\sim 10^{-3}$  torr. The specifications of the spectrometer are: Rigidity of the magnet = 0.045 Kg-m, Resolution  $\sim 7\%$ , transmission  $\sim 10^{-3}$ . The spectrometer was tested with Cs-137 beta source and the spectrum is shown in following figure.



## 2.4.9 Development of Spark Counter

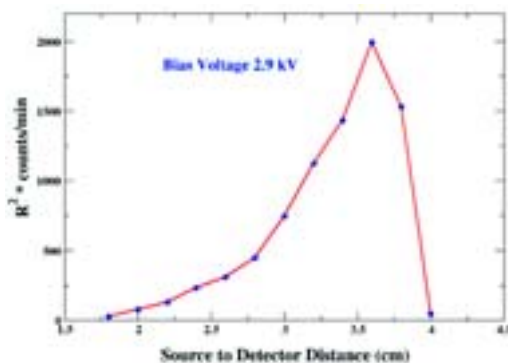
A. Mandal, S.K. Saini, Rajesh Kumar, S.K. Suman and S.K. Datta

A project has been taken to develop an instrument to study the ionizing effect of radioactivity for M. Sc. Teaching course. When a high voltage is applied in a spark chamber (between ground plane and copper wire kept 1mm apart) and a radioactive source is brought near to high voltage applied on thin wire, the air gap between ground plane and HV wire is ionised due to creation of avalanche electron. This forms a discharge path for high voltage, and generates sparks where particles pass. A complete assembly consists of spark chamber, high voltage power supply and a pulse counter.

*Spark chamber:* It is a chamber made of insulated material housing two electrodes an aluminum plate and a thin nicrom wire. A positive voltage is applied to wire. This chamber also has an adjustable arrangement to hold the radioactive source.

*High voltage power supply:* A 0-5kV supply provides the bias voltage. The supply uses a DC to DC converter to charge a Cockroft Walton multiplier circuit. The primary of step up transformer is driven from the SMPS control circuit operated at 20 KHz. The output voltage is adjusted by controlling the voltage applied to the primary of the transformer.

*Pulse counter:* Whenever there is a spark in spark chamber, it draws large current from HV power supply for the duration of spark. The large current pulses are passed through a resistance mounted in series of the load, and this way corresponding voltage pulses are obtained for every spark. These pulses are counted by a counter.



These three parts have been integrated together in a single cabinet and the same instrument can be utilized for control of the Beta spectrometer as well as for control of other detectors. The response of the spark counter with the source to detector distance was measured with an Am-241 source. The response curve is shown in the figure. This curve can be used to measure range of alpha particles in air. The performance of the instrument was demonstrated in the teaching workshop.

#### 2.4.10 Beam Hall Activities

P. Barua, A. Kothari and A. Mandal

Different activities in beam hall-II are summarized.

##### Beam line installation-

- Installation of – 40 degree (GPSC) beamline complete
- Changing leaky beam pipe of quadrupole magnet in GPSC beamline in BH-II.
- Complete Installation of Material Science and Atomic Physics Beam lines
- Remote connection of all beam line components to control room complete
- Beamline tested with O-16 beam and successful transmission of pelletron beam to targets in BH-II

**Cable tray layout-** The trays for cabling to Data room and control room have been mounted.

**Water line-** The piping for cooling water up to different beamlines has been completed. Experimental facilities will be covered as and when need. Water line in INGA-HYRA area is being extended to provide cooling water to HYRA magnets and power supplies.



## 2.5 LOW ENERGY ION BEAM FACILITY (LEIBF)

G. Rodrigues, P. Kumar, P.S. Lakshmy, U.K. Rao, Y. Mathur, S. Kumar, C.P. Safvan and D. Kanjilal

The ECR source on 300 kV platform has been running satisfactorily during the last year. The extraction system was modified to bring the source closer to the Einzel lens in order to reduce the drift and also to bring the puller electrode closer to the plasma electrode keeping other dimensions unaltered. Calculations using IGUN predicted that in the original extraction configuration, significant loss in the beam intensity and poor electric focusing was very apparent. Therefore, this step was taken to get the optics in a better way. Indeed after a comparison, the new system worked out quite well. We could get analyzed beams of 175  $\mu\text{A}$  of  $\text{H}^+$  and 300  $\mu\text{A}$  of  $\text{H}_2^+$  during a typical MIVOC run at low RF power as compared to earlier cases of achieving a few  $\mu\text{A}$  with the old configuration. In another comparison using Argon beam, it was clear that the transmission of the low charge states were much better as compared to the higher charge states. The experiments are being carried out to improve this situation further, except that the current limitation will come mainly from the current rating of the high voltage deck power supply which has a maximum value of 2 mA.

New metal beams like Ni and Eu were developed. Nickel which is a difficult beam like Fe was extracted (using the new extraction system) using nickelocene ( $\text{Ni}(\text{C}_5\text{H}_5)_2$ , a Metal Ion using Volatile Compound, [MIVOC]) with the material placed inside the 'floating' bias tube so that the metal vapours have a higher probability of getting ionized near to the ECR zone than sticking to the cold wall of the chamber. We found that this technique has definite gains over the conventional way of placing the MIVOC compound in a separate chamber connected to the source, although the bias tube was not being polarized which is normally done in other sources. After some experience and discussions with colleagues in other laboratories it was realized that the bias tube needs to be polarized while using the MIVOC technique. This idea is currently being worked upon and will be implemented soon. A typical spectrum showing the charge state distribution of  $^{58}\text{Ni}$  is shown in figure 1. below.

Plans are going on to shift the existing facility to the new building in view of the developments going on in Beam Hall II and also to have a complete full fledged facility in terms of operation of the facility at 400 kV/q within a larger space area. The complete design has been worked out and fabrication of new high voltage, double deck platform are already underway. Two additional beam-lines are planned and this requires a new switching magnet for this purpose. The new modifications in the system will be ; (a) to have a magnetic quadrupole doublet (instead of an Einzel lens) after the source extraction to get better focussing and an additional strong focussing lens immediately after the acceleration tube ; (b) additional pumping on the injection side of Nanogan will be worked out in order to get better vacuum and better pumping on the extraction side at least for improvement of the output of highly charged ions ; (c) gas injection will be done through

the bias tube in order to save expensive gases and (d) extraction system will be modified and integrated with the magnetic quadrupole doublet.

A test set-up has been established for off-line testing of TWTA microwave amplifiers. Indigenisation of TWT modules has been taken up. Corresponding power and high voltage modules have been tested. One of our spare TWT amplifiers was found to have non-linearity and reflected power read-back problems. Its corresponding solid state amplifier was modified to improve the linearity and the old detector was replaced with a new one for obtaining the reflected power read-outs.

A light link interface was designed and developed for the requirements of High Current Injector and Low Energy Ion Beam Facility. It is primarily based on V/F conversion using IC AD650 (V/F and F/V) and Agilent's HFBR1523, HFBR2523 transmitter and receivers respectively. AD650 works on the charge balancing principle. The module has been tested and will be used for the 'soft-landing' system.

For experiments related to ion-gas target interactions, it was realized that proper collimation of beam before the gas target was very important. Therefore, the two such collimators before gas target were carefully aligned by taking the reference of analyzing magnet. The post analyzer section was re-aligned with special care to beam profile monitor (BPM), double slits and electrostatic quadrupole triplet. This re-alignment delivered good quality beam for the ion gas-target interaction experiments and good quality data were

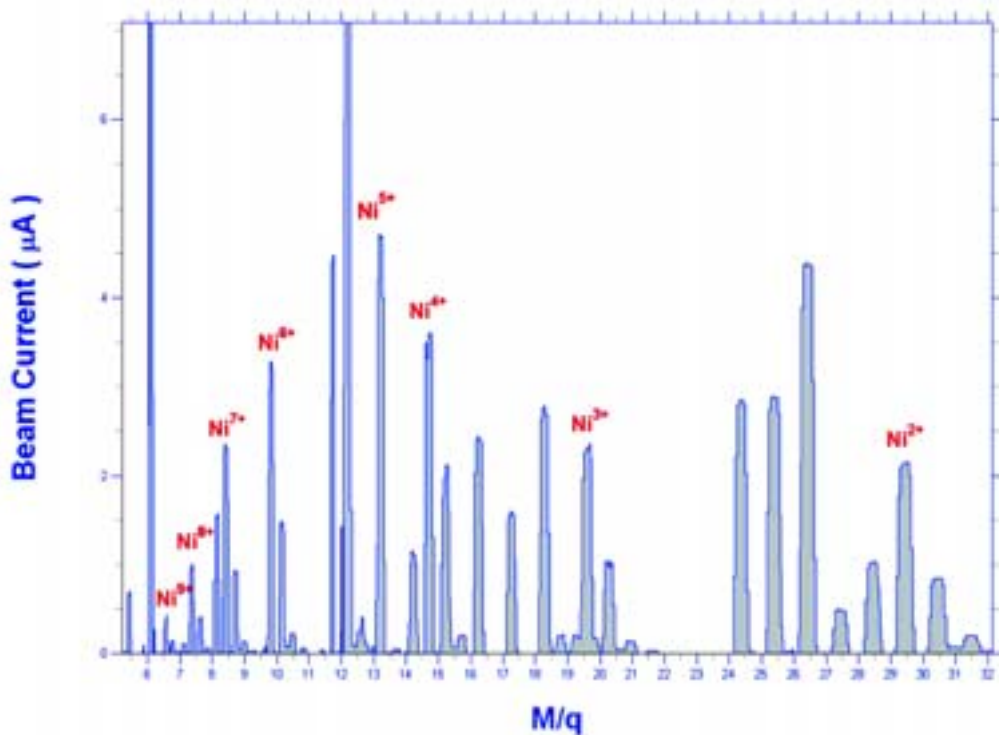


**Fig. 1. Charge state distribution optimized on  $^{58}\text{Ni}^{4+}$**

recorded, which was never possible earlier. This gave new exciting results for the experiments.

The Low Energy Ion Beam Facility has been running almost full time for various experiments during the last year. A list of some of the experiments performed using LEIBF beams is given in table 1 below. We have been developing in-depth expertise in various modes of operation of ECR ion source and developing newer beams. Various experiments of atomic and molecular physics and materials science are being carried out during the operation of LEIBF.

**Table 1. List of experiments performed in the Low Energy Ion Beam Facility (LEIBF) in 2005**

Experiment	Beam	Dose (particles/cm <sup>2</sup> )	Energy
Implantation of N on GaAs substrate to see GaN phase formation	N <sup>+</sup>	1.0 x 10 <sup>18</sup>	50 keV, 130 keV, 290 keV
Formation of ZnO nano-particles in quartz matrix using Zn beam	Zn <sup>2+</sup>	1 x 10 <sup>16</sup> , 5 x 10 <sup>16</sup> , 1 x 10 <sup>17</sup>	200 keV
Effect of Ar implantation on Au/'n' type Si Schottky barrier Implantation of Eu on Zn implanted and annealed quartz and ZnO films in order to dope ZnO nano-particles embedded in SiO <sub>2</sub>	Ar <sup>153</sup> Eu <sup>4+</sup>	1.0 x 10 <sup>11</sup> 1.0 x 10 <sup>15</sup> , 2.0 x 10 <sup>15</sup>	1 MeV 375 keV
Testing of TOF set-up using N on Ar target	N <sup>5+</sup>	—	100 keV
Experiments with ethanol droplets to probe density effects	N <sup>1+ to 5+</sup>	—	100 kV/q, 150 kV/q
To study electrical and optical properties of SiN, quartz, polymers, ZnO and CuO samples on Ni implantation	Ni <sup>2+</sup>	—	200 keV
Study of optical properties of Eu doped SiC and quartz	Eu <sup>3+</sup>	2 x 10 <sup>15</sup> , 5 x 10 <sup>15</sup> , 1 x 10 <sup>16</sup>	300 keV
C implantation of Si matrix to study formation of embedded SiC precipitates	C <sup>+</sup>	3 x 10 <sup>17</sup> , 6 x 10 <sup>17</sup>	50 keV, 150 keV
Study of effect of Ar beam on polymer matrix to reduce cluster size	Ar <sup>+</sup>	—	60 keV

Experiment	Beam	Dose (particles/cm <sup>2</sup> )	Energy
Ion irradiation effects on optical properties of SiC thin films	Ar <sup>+</sup>	—	150 keV
Implantation of Si samples for performing TCR measurements for device purposes	C <sup>+</sup> , C <sup>2+</sup>	5 x 10 <sup>16</sup>	100 keV, 200 keV
Implantation of Ar on 500 nm C <sub>60</sub> films	Ar <sup>2+</sup>	1 x 10 <sup>13</sup> , 1 x 10 <sup>14</sup> , 1 x 10 <sup>15</sup> , 1 x 10 <sup>16</sup> , 5 x 10 <sup>16</sup>	250 keV
Testing of TOF for multi-hit coincidence timing using Ar on targets of Ar, N <sub>2</sub> , C <sub>2</sub> H <sub>2</sub> , CH <sub>4</sub> , CH <sub>3</sub> OH, C <sub>2</sub> H <sub>5</sub> OH, CH <sub>3</sub> OD	Ar <sup>8+</sup>	—	1.2 MeV
Studies on Ion-molecule interactions using Ar	Ar <sup>q+</sup>	—	150 kV/q
Study of magnetic interaction in different matrices and different phase formation under different treatments and annealing and heavy ion irradiation on quartz, SiO <sub>2</sub> /Si and C <sub>60</sub> /Si samples	Fe <sup>+</sup>	1 x 10 <sup>13</sup> , 1 x 10 <sup>14</sup> , 1 x 10 <sup>15</sup> , 1 x 10 <sup>16</sup>	150 keV
Synthesization of iron based Si/GaAs nanoclusters	Fe <sup>3+</sup>	1 x 10 <sup>14</sup> , 1 x 10 <sup>15</sup> , 1 x 10 <sup>16</sup> , 5 x 10 <sup>16</sup>	200 keV
Fabrication of nano-dots and nano-ripples on GaAs, InP and Si samples and study of morphological investigation by SEM, AFM and optical properties by Raman and PL spectroscopy	Ar <sup>+</sup>	1 x 10 <sup>17</sup> to 1 x 10 <sup>18</sup>	50 keV, 100 keV

## 2.6 PERFORMANCE OF HIGH TEMPERATURE SUPERCONDUCTING ECRIS AND LOW ENERGY BEAM TRANSPORT SYSTEM

G. Rodrigues, P. Kumar, P.S. Lakshmy, U.K. Rao, Y. Mathur, A. Mandal, D. Kanjilal and A. Roy

The First High Temperature Superconducting Electron Cyclotron Resonance Ion Source (HTS-ECRIS) called PKDELIS operational at both 14.5 and 18 GHz has been installed.

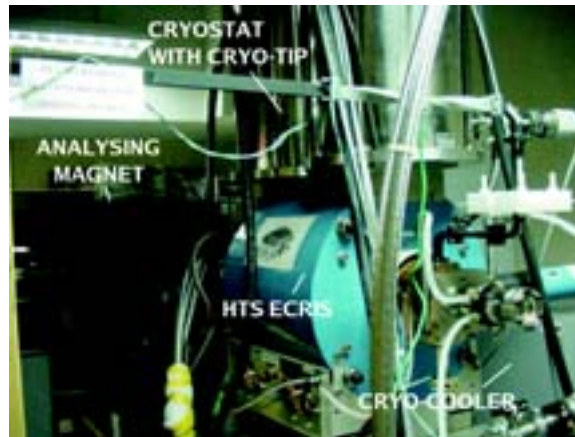


**Fig. 1. View of the installed HTS ECR ion source and analysing magnet**

A view of the HTS (Bi-2223) ECR ion source and related components installed at ground potential is shown in figure 1. The HTS coils are housed in separate cryostats. The HTS coils are cooled to below 23 K for optimum operation and have been working satisfactorily. The source is powered by a 18 GHz, 1.7 kW klystron generator. The plasma chamber and the bias tube is water cooled using a dedicated, portable, closed cycle water cooling system. If the temperature or the water flow rate does not conform to within specified limits, the RF generator will be forced to shut down to protect the plasma chamber and the permanent magnets of the hexapole. A small, medium resolution, large acceptance, air-cooled, 90° analysing magnet has been installed and coupled close to the source. The aperture and radius of the magnet was chosen to be 80 mm and 300 mm respectively. A multi-electrode, air cooled extraction system has been coupled between the source and the analysing magnet with a pumping port installed just after the extraction system. It consists of three cylindrical electrodes, which can be biased properly to achieve reasonable transmission and mass resolution. A 1 kW water-cooled Faraday cup is used for measuring the analysed beam currents. The entire beam-line was tried to be made as short as possible with as few diagnostic elements as possible in order to avoid loss in the beam intensity. A schematic view of the low energy beam transport system is shown in figure 2. The x-ray radiation levels around the source were measured at different coil currents in the HTS coils

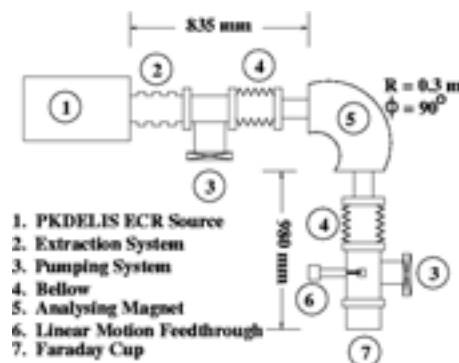


**Fig. 2. Schematic of the Low Energy Beam Transport System**

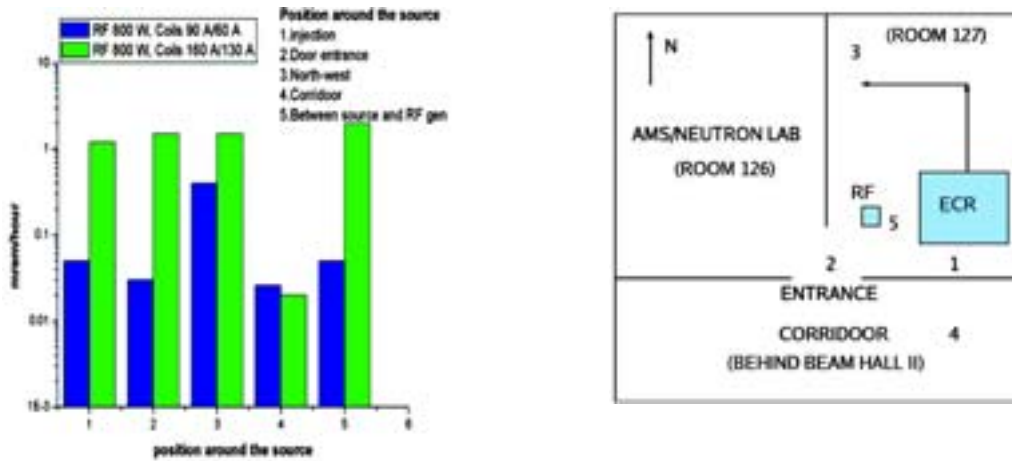


**Fig. 3. Radiation levels measured with Pb shielding around the source**

and RF power levels. At relatively higher coil currents and RF power levels of the order of 500 W, the radiation levels were maximum on the extraction side and measured to be of the order of 7 rad/hour. In order to be in the safe working limit during regular operations, lead shielding structures around and close to the source were designed and positioned close to the source. After the installation of these shielding structures, the radiation levels were measured again to verify the design. This is shown in figure 3.

The extraction current measurements were determined for  $\text{Ar}^{8+}$  and  $\text{Ar}^{12+}$  beams. Figure 4 (a) shows the transmission of these beams measured at 10 Watts of RF power with coil currents set at 130 A and 120 A on the injection and extraction coils respectively. Figure 4 (b) shows the charge state distributions typical for argon at two different coil current settings measured at lowest RF power level of 10 Watts. At lowest power levels of 10 Watts and at a particular setting of the coil currents, the peak of the distribution shifts to  $\text{Ar}^{8+}$ . Although the source is able to produce huge amounts of currents from the experiences of the first tests, the beam transport section has to be further optimized. From optics point of view, the distance 'd' of the faraday cup is presently more than the required 2R position. Therefore, loss in the beam at the faraday cup is as expected.

A new, movable type, high current extraction system is presently under fabrication. This will facilitate in tuning the optics of various A/q beams under the influence of the strong axial magnetic field. The electrodes will be water cooled using de-ionized water. The pumping system will be mounted on the extraction tank to facilitate better vacuum close to the beam formation region. A series of ports will be mounted on the extraction tank body, one of them will be used for mounting a variable energy electron gun to study the effect of space charge neutralization and alternately, another could be used to inject electro-negative gases into the system. This concept needs a careful study in order to limit the beam emittance. From simulations, it has been verified that the emittance can be reduced from  $150 \pi \text{ mm.mrad}$  to  $100 \pi \text{ mm.mrad}$  depending on the space charge neutralization fraction and the electron energy. An artist impression of the system is shown in figure 5.

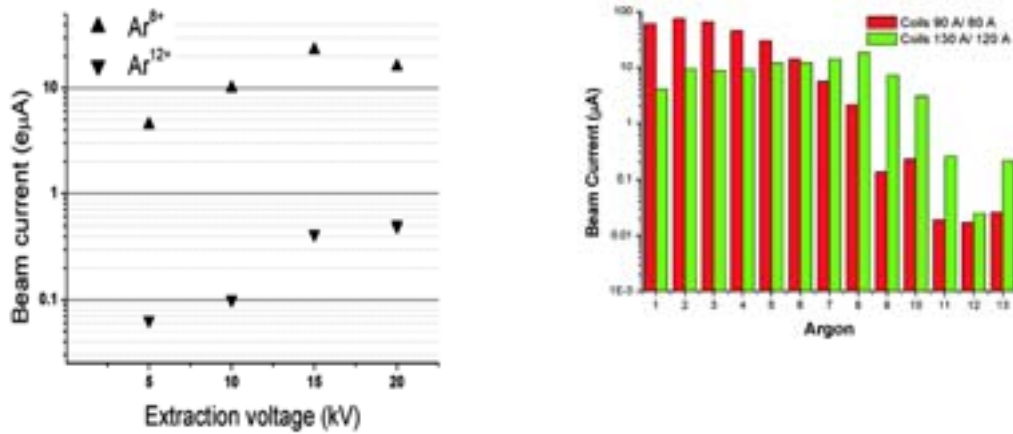


**Fig. 4. (a) Extracted currents; (b) Charge state distribution for argon**

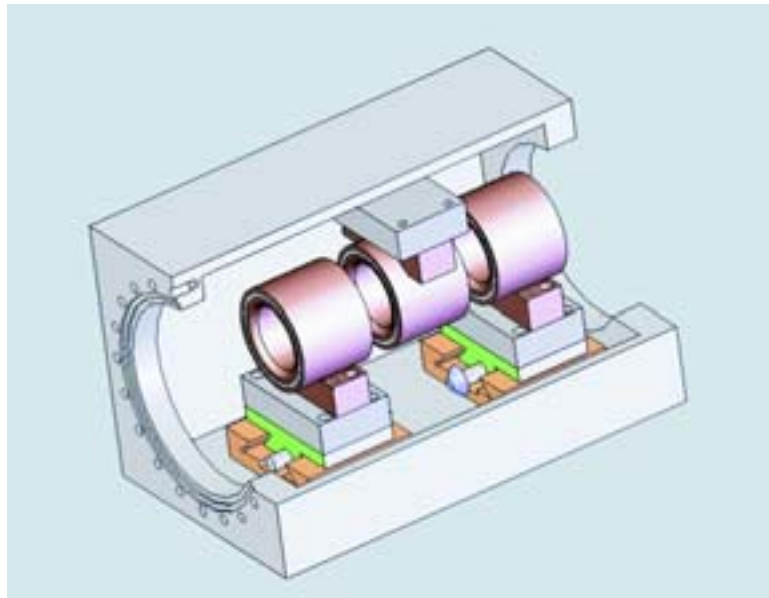


**Fig. 5. An artist's impression of the new water-cooled, high current extraction system**

A minor problem had occurred during regular operations with the system, i. e., one of the cryo-coolers (extraction side) could not cool-down the cold head to temperatures close to 23 K in a normal time of 10 to 12 hours. This limited the source from operating in the normal manner. We suspected that the He got contaminated using 10 ppm of He earlier. Apparently, the helium gas was also found to be leaking. This leak was rectified. All the individual components viz., cold head, flex lines, adsorber and compressor were evacuated and recharged separately using 1 ppm level of He. The cryo-cooler is working fine and the HTS ECR is working satisfactorily using this cryo-cooler.



## 2.7 BEAM OPTICAL DESIGN AND FABRICATION OF PROTOTYPE RFQ ACCELERATOR STRUCTURE FOR HIGH CURRENT INJECTOR

C.P. Safvan, Sugam Kumar, R. Ahuja, A. Kothari, D.Kanjilal and Amit Roy

A room temperature Radio Frequency Quadrupole (RFQ) accelerator has been designed and a prototype has been fabricated to accelerate the ions from the ECR ion source. The accelerator has been designed to accept charged particles of mass by charge ratio of 7. The RFQ will accelerate and bunch these beam to 150keV/u which will be further accelerated by a Drift Tube Linac (DTL) being designed at TRUIMF. The RFQ will operate at 48.5MHz (a sub-harmonic frequency of 97MHz at which existing superconducting LINAC will be running).

Radio Frequency cavity structure simulations have been carried out using Microwave Studio to design an easily machinable cavity that resonates at 48.5MHz, keeping nearby RF mode spacing as far as possible. The final structure is a combination of the features of already existing RFQ accelerator, most notably the CERN REX-ISOLDE and the RIKEN RFQ's.

Beam Optics simulations to determine the detailed vane structure of the RFQ accelerator, and to investigate the beam dynamics (energetic and emittance growth, tolerance to beam misalignments) for 300keV/u was done and simulations for 150keV/u using standard software like LIDOS is under process.

For prototype RFQ the final Cavity structure has been fabricated at Donbosco Technical Institute's Workshop. The unmodulated Vane and Vane Supports were successfully manufactured at Indo German Tool Room Indore and Ahemdabad respectively. The vacuum leak testing of cavity has been done and system is ready for vanes alignment to measure the RF properties like resonant frequency, tunability, Q-value, field uniformity and mechanical properties like stability and water cooling systems.

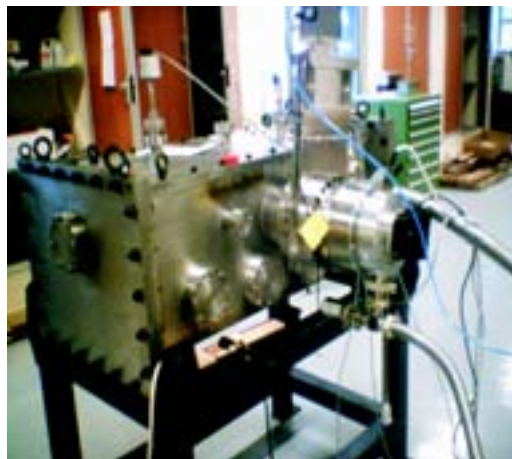


**Fig. 1. Prototype RFQ Cavity structure**